AIP | Journal of Applied Physics

Optical properties of GaAs/GaP strainedlayer superlattices

M. Recio, G. Armelles, J. Meléndez, and F. Briones

Citation: J. Appl. Phys. 67, 2044 (1990); doi: 10.1063/1.345588
View online: http://dx.doi.org/10.1063/1.345588
View Table of Contents: http://jap.aip.org/resource/1/JAPIAU/v67/i4
Published by the American Institute of Physics.

Related Articles

Visible light emission and energy transfer processes in Sm-doped nitride films
J. Appl. Phys. 111, 123105 (2012)

Structural and optical properties of InAs/AlAsSb quantum dots with GaAs(Sb) cladding layers
Appl. Phys. Lett. 100, 243108 (2012)

The electronic band structure of GaBiAs/GaAs layers: Influence of strain and band anti-crossing
J. Appl. Phys. 111, 113108 (2012)

Growth of AlN/SiC/AlN quantum wells on Si(111) by molecular beam epitaxy
Appl. Phys. Lett. 100, 232112 (2012)

Time-resolved photoluminescence, positron annihilation, and Al0.23Ga0.77N/GaN heterostructure growth studies on low defect density polar and nonpolar freestanding GaN substrates grown by hydride vapor phase epitaxy
J. Appl. Phys. 111, 103518 (2012)

Additional information on J. Appl. Phys.

Journal Homepage: http://jap.aip.org/
Journal Information: http://jap.aip.org/about/about_the_journal
Top downloads: http://jap.aip.org/features/most_downloaded
Information for Authors: http://jap.aip.org/authors

ADVERTISEMENT

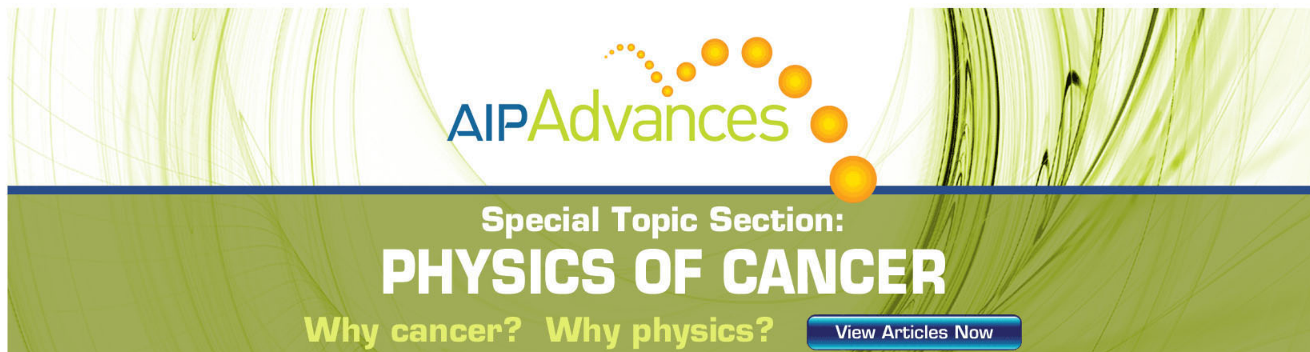

Downloaded 27 Jun 2012 to 161.111.180.103. Redistribution subject to AIP license or copyright; see http://jap.aip.org/about/rights_and_permissions

Optical properties of GaAs/GaP strained-layer superlattices

M. Recio, G. Armelles, J. Meléndez, and F. Briones
Centro Nacional de Microelectrónica, Consejo Superior de Investigaciones Científicas, Serrano 144, 28006 Madrid, Spain

(Received 19 July 1989; accepted for publication 4 November 1989)

The optical properties of a novel system, the GaAs/GaP strained-layer superlattice, are studied and compared with a theoretical model. Photoluminescence and photoreflectance measurements revealed that among the set of superlattices under study type-I and type-II behaviors (similar to those found in the lattice-matched GaAs/AlAs system) are present. The evolution of the photoluminescence peaks as a function of temperature and excitation density supported the assignment of the transitions involved. This is to our knowledge the first observation of direct (type-I) and indirect (type-II) transitions in strained-layer superlattices. A comparison with a theoretical model has led to an estimation of the conduction-band offset as 0.4 eV, which is the first value obtained from experiment in a GaAs/GaP heterojunction.

I. INTRODUCTION

Semiconductor heterostructures made of lattice-mismatched materials have lately received considerable attention for several reasons: basic research interest in the role of the stress on the electronic structure and lattice dynamics[1] and technological applications such as enhancing the choice of materials for heterostructure devices[2] and buffers for growing on Si substrates and new transport properties due to strain-induced band splitting.[4]

Recent advances in epitaxial growth techniques have allowed growth of good-quality strained-layer superlattices (SSL), with the restriction that the constituent layers must be "thin enough" in order to accommodate by elastic deformation the strain due to the mismatch. Therefore optical studies again become (as in lattice-matched materials) of primary interest. Theoretical predictions of the reliability of strained-layer superlattices were proposed and Marzin and Gerard[1] in relation to the tailoring of various superlattice electronic optical and structural properties. In particular, for superlattices containing GaP the only system studied so far has been $GaP/GaAs_xP_{1-x}$ $(0<x<.6)$ on GaP substrates where the theoretical predictions have been confirmed by measuring optical transitions.[5]

We have grown and characterized GaAs/GaP strained-layer superlattices grown on GaAs substrates. In principle, optical and electrical characteristics of this system should be similar to those of GaAs/AlAs because both are composed of one direct and one indirect material. However, strain, as a new parameter appearing in these superlattices, will modify substantially the optical properties and band structure.

Again in these SSL one can find that, for certain layer thicknesses and strain levels, the lowest confined electron state of the system comes from the X minimum of GaP, and therefore we will have superlattices with electrons confined in GaP layers and holes in the GaAs layers, giving rise to indirect (in real space) transitions. In the following, we will call them type-II superlattices. On the other hand, we will call type-I superlattices those in which electrons and holes at their lowest energy level are located in the GaAs layers, giving rise to direct transitions.

For this kind of superlattice in which direct (type I) and spatially indirect (type-II) behaviors are expected, the combination of an emission-related technique and an absorption-related technique has been extensively used[6] in order to delve into the origin of the observed transitions.

The reason for this is related mainly to the very small oscillator strength of the lowest-energy transitions in type-II superlattices due to the small overlapping of the electron and hole wave functions. In these type-II superlattices, two different kinds of transitions are observed: The lowest-energy transition (which is the spatially indirect one) is observed by means of the emission-related technique, while the lowest direct transitions are observed with the absorption-related technique.

The lineup of the bands at the heterointerface that determines the barrier height for electrons and holes is of extreme interest from the physical point of view and of importance for applications based on the GaAs/GaP system. Therefore we were interested in determining the band offset of the GaAs/GaP junction.

In the present paper, we report on optical characterization of short-period GaAs/GaP strained-layer superlattices grown by atomic layer molecular-beam epitaxy (ALMBE) on GaAs substrates. Photoreflectance (PR) (absorption-related) and photoluminescence (PL) (emission-related) spectroscopies are used to obtain the energies of the different transitions. The evolution of the spectra with variable temperature and excitation power was followed in order to identify the various transitions observed. Moreover, electron transfer effects assisted by a temperature increase in type-II superlattices are observed in the PL spectra between the lowest indirect and the lowest direct transitions, similar to what occurs in AlAs/GaAs type-II superlattices.[7]

The energies of the transitions are compared with a four-band-envelope wave-function model in which strain effects and remote band coupling are taken into account. In type-II superlattices a Kronig-Penney model with continuity in effective masses and including stress effects is used for the calculation of the conduction-band states. The value of the strain used in this calculation was deduced from Raman measurements as detailed in Ref. 8. The only adjustable pa-

 0021-8979/90/042044-07$03.00 © 1990 American Institute of Physics

Downloaded 27 Jun 2012 to 161.111.180.103. Redistribution subject to AIP license or copyright; see http://jap.aip.org/about/rights_and_permissions

rameter is then the band offset and, therefore its value can be deduced by means of the comparison between calculated and experimentally observed transitions.

We have also studied and calculated the optical properties of structures consisting of two GaAs/GaP superlattices confining GaAs quantum well (16 monolayers thick). From the observed transitions originating in the superlattices and in the quantum well additional experimental data are used to estimate the band offset.

II. EXPERIMENT

Two different sets of samples were grown for this study. In Table I their parameters (superlattice period, composition, and accommodated strain in the layers) are presented. Samples M1, M2, and M3 are GaAs/GaP superlattices with different slab thicknesses of their constituent materials. Samples M4, M5, and M6 are structures consisting of two GaAs/Gap superlattices confining a quantum well of 16 monolayers.

Samples are grown by a new technique developed in our laboratory (ALMBE),[9] at a substrate temperature of 425 °C. X-ray diffraction and Auger electron spectroscopy (AES) measurements provided structural characterization of the samples (total period d and the thicknesses of the constituent layers d_{GaAs} and d_{GaP}). Raman scattering was performed to obtain the strain level accommodated in the GaAs and GaP layers.

All the parameters from the samples are displayed in Table I. For PL measurements, the samples were placed in a variable-temperature cryostat cooled by liquid helium, using as an excitation beam the 488.0-nm line of an Ar^+ laser. Emitted light was analyzed with a double monochromator and a cooled GaAs photomultiplier, coupled with a photon-counting system. For PR measurements, which gave information on absorption transitions, the samples were illuminated with a halogen lamp, and the reflected light was analyzed with a 0.3-m focal length spectrometer and a Si photodiode. Sample reflectivity was modulated by means of an Ar-laser beam chopped at 510 counts/s. We have used the three-point method[10] to determine the energies of the PR transitions.

TABLE I. Superlattice parameters: d_{GaAs} and d_{GaP} are slab thicknesses and ϵ_1 and ϵ_2 the strains accommodated in the GaAs and GaP layers, respectively. The total thickness of the SSL in samples M1, M2, and M3 is 0.4 μm, while that of the two confining SSL in samples M4, M5, and M6 is 0.2 μm.

Sample	Period (Å)	d_{GaAs} (Å)	d_{GaP} (Å)	ϵ_{GaAs} (%)	ϵ_{GaP} (%)
M1	22.3	16.7	5.6	0	3.7
M2	27.2	16.2	11.0	0.7	3.0
M3	32.4	18.4	14.0	1.4	2.3
M4	33.3	18.6	14.7	0.7	3.0
M5	26.1	16.5	9.6	0	3.7
M6	24.5	17.0	7.5	0.3	3.4

III. RESULTS

A. Samples M1, M2, and M3

As exposed, the optical characterization of the samples has been carried out by PR and PL measurements in the range 4–300 K. In the PR spectra, several direct (Γ-Γ) transitions from the superlattice will be observed, namely, conduction-band (CB)–heavy-hole band (HH), CB–light-hole (LH), and CB–split-off band (SO). In some samples, the transitions of HH and LH are not resolved, and the experimental energy of both cannot be accurately established.

In PL spectra, the lowest-energy transitions are observed, but if the lifetime of the electrons in this lowest level is high enough, saturation of this level may occur due to an increase of population assisted by an increase in temperature or excitation density. In this last situation, higher-energy transitions with shorter lifetimes may appear in the photoluminescence spectrum. This is true for the X transitions in type-II superlattices, because they have lifetimes that are orders of magnitude longer than the Γ transitions which are higher in energy.[7]

At 4 K only one peak (labeled A) in the spectra from samples M2 and M3 could be observed in the PL spectra at any excitation intensity. The energy of the transition associated with peak A does not correspond with the lowest observed PR transition. Consequently, we started thinking about type-II behavior in these particular samples (the recombination is spatially indirect, the electron and hole wavefunction overlapping is small, and therefore the associated transition will not appear in the PR spectrum).

In Fig. 1 we present the PR and PL spectra for each sample M1, M2, and M3 at 70 K. A second peak (labeled B) is clearly observed in the PL spectra of samples M2 and M3. As can be seen from Fig. 1, in sample M1 the energy of the observed PR superlattice transition corresponds to the lowest transition observed in PL, so that it must have a direct character, and thus the GaAs layers are well for both electrons and holes at the same time.

On the other hand, in samples M2 and M3 we observe with PL a transition at 1.73 eV in both samples (peak A), while with PR the lowest SL transition lies at 1.81 eV (peak B in sample M2) and 1.865 eV (peak B in sample M3). Therefore in these samples, the transitions associated with peaks A must have a very small probability, as would correspond to type-II transitions as indicated before. The peaks labeled B in PL and the lowest superlattice transitions observed by PR lie at the same energy, and must have a high probability, which would correspond to a direct type-I transition in the GaAs layers. All these facts support the assignment of type-I superlattice to sample M1 and type-II superlattices to samples M2 and M3.

In order to test the possible type-II origin of peak A in samples M2 and M3 we have studied the PL dependence with temperature and excitation power. Similar studies have been already reported for the unstrained GaAs/AlAs system.[11] In Fig. 2, we present the evolution of the PL spectra from sample M2 when the temperature is raised (at constant excitation power) from 4 to 160 K. At 4 K only peak A is observed, but as we raise the temperature, a second peak

Downloaded 27 Jun 2012 to 161.111.180.103. Redistribution subject to AIP license or copyright; see http://jap.aip.org/about/rights_and_permissions

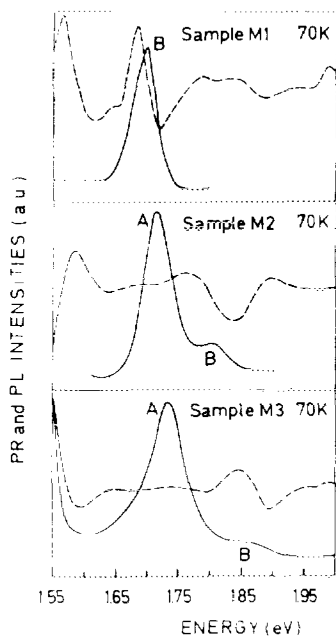

FIG. 1. PR and PL spectra from samples M1, M2, and M3 in Table I. In sample M1, both PR and PL transitions take place at the same energy. In samples M2 and M3, the main transition observed by PL lies at lower energy than the PR transition, which coincides with a weaker PL peak labeled B.

(labeled B) appears on the high-energy side of the former peak. If the temperature is raised further, both peaks become equally intense, and at 160 K only peak B is observed.

One can derive from the spectra that as the temperature is increased, saturation with the temperature of peak A, originating from the conduction-band level, is eventually reached, as well as the population of peak B, originating from a higher level. These band-filling effects are related to the long lifetimes in the lowest level and shorter lifetimes in the higher level. In particular, these effects have been observed in GaAs/AlAs type-II superlattices where the lifetime of electrons in the confined X AlAs state is much higher than the lifetime in the higher-energy confined Γ GaAs state.[7]

From the evolution energy of the peaks as a function of the temperature, more information about the origin of the transitions can be achieved. The rate of increase (q) in the emission energy is different for different transitions. Peak A shifts much more slowly ($q \sim 2KT$) with increasing temperature than peak B, which has a rate of increase in emission energy ($q \sim 1/2\ KT$) equivalent to that of the GaAs direct band of the band gap. Similar results have recently been found for type-II GaAs/AlAs superlattices.[11]

In Fig. 3, we present several PL spectra at different excitation intensity conditions. Peak A saturates and peak B is only observed when the power is high enough. Again this effect is attributed to population of the Γ level in GaAs layers and to the filling of X-levels of GaP. The shift in the energy of peak B is related to a local heating of the sample (temperature effects) that would also contribute to a faster evolution in the filling of the Γ state.

Similar behavior for the dependence with temperature and excitation intensity is found in sample M3, but in this sample, peak B does not grow as quickly as in sample M2. The cause of this can be found in the higher energy distance between the two involved conduction-band states. The energy distance between peaks A and B is ~ 130 meV for sample M3 and ~ 80 meV for sample M2.

All these facts are in good agreement with the assignment of a type-I transition to the peaks labeled B and a type-II transition to the peaks labeled A.

The broadness of the peaks observed in the PL spectra of all three samples is affected by monolayer fluctuations in the layer thickness and strain gradients in the growth direction due to the relaxation from the substrate. Analogously, the PR spectra show broad peaks in which the direct transitions to the light-hole and heavy-hole bands cannot be accurately determined, and only an approximated estimation can be made. The transition to the split-off band of the superlattice is observed by PR in all three samples (see Fig. 4).

All the energies experimentally obtained in PL and PR of the different transitions are displayed in Table II. PL ex-

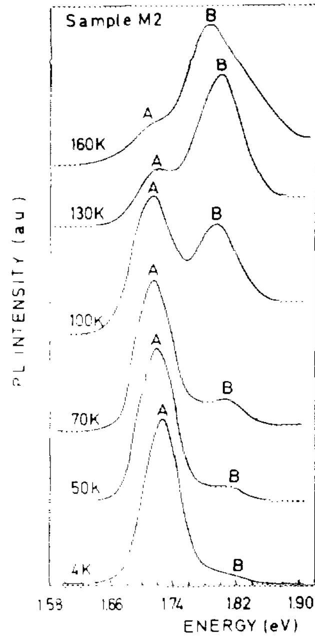

FIG. 2. Temperature dependence of the PL spectrum of sample M2.

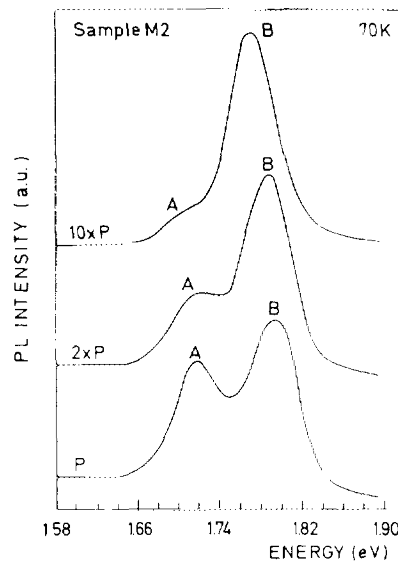

FIG. 3. Excitation density dependence of the PL spectrum of sample M2.

Downloaded 27 Jun 2012 to 161.111.180.103. Redistribution subject to AIP license or copyright; see http://jap.aip.org/about/rights_and_permissions

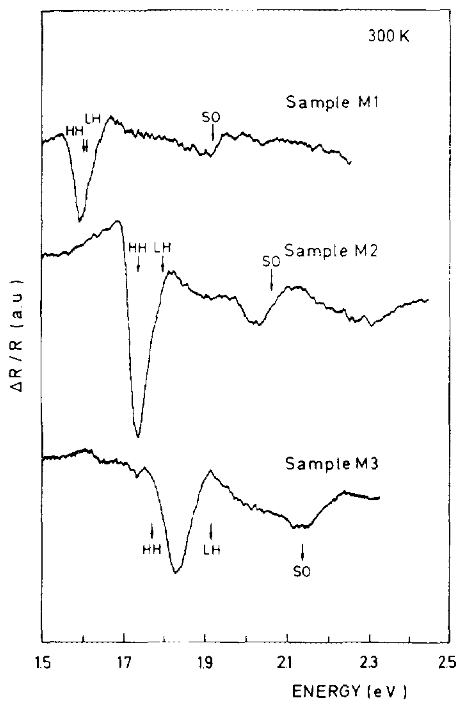

FIG 4. PR spectra from samples M1, M2, and M3. Arrows indicate the calculated energies for the HH, LH, and SO transitions (translated to 300 K by substracting 96 meV).

periments under hydrostatic pressure are currently being carried out for these samples, and preliminary results are in good agreement with type-I and type-II assignments for peaks B and A, respectively.

B. Samples M4, M5, and M6

In this set of samples, a 16-monolayer-thick GaAs quantum well (QW) is confined by two GaAs/GaP superlattices

TABLE II. Energies of the PL and PR observed transitions together with the results of the calculations for conduction-band offsets (CBO) of 0.3, 0.4, and 0.5 eV. HH is the conduction-band–heavy-hole transition, LH the conduction-band–light-hole transition, SO the conduction-band–spin-orbit split-off band transition, and II the lowest type-II transition. The temperature is 4 K. PR values correspond to the energy of the transitions obtained at 300 K plus the 96-meV thermal gap shift of GaAs from 300 to 4 K.

Sample	PL (eV)	PR (eV)	Calculation CBO = 0.3 (eV)	CBO = 0.4 (eV)	CBO = 0.5 (eV)
M1	1.690	1.705	HH 1.699	HH 1.714	HH 1.727
		2.000	LH 1.713	LH 1.717	LH 1.717
			SO 2.016	SO 2.021	SO 2.023
			II 1.653	II 1.750	II 1.838
M2	1.730	1.830	HH 1.800	HH 1.830	HH 1.849
	1.810	2.170	LH 1.909	LH 1.918	LH 1.920
			SO 2.164	SO 2.175	SO 2.181
			II 1.660	II 1.750	II 1.857
M3	1.730	1.867	HH 1.837	HH 1.856	HH 1.887
	1.860	2.250	LH 2.009	LH 2.019	LH 2.019
			SO 2.224	SO 2.240	SO 2.249
			II 1.672	II 1.740	II 1.832

TABLE III. Energies of the PL and PR observed transitions together with the results of the calculations for a conduction-band offset (CBO) of 0.4 eV. QW denotes the quantum well, SL the superlattice, HH the conduction-band–heavy-hole band transition, LH the conduction-band–light-hole band transition, II the lowest type-II transition. The temperature is 4 K. PR values are obtained as described in Table II.

Sample	PL (eV)	PR (eV)	Calculation CBO = 0.4 eV (eV)
M4	QW 1.675	QW 1.665	QW 1.661
			HH 1.8166
	SL 1.748	SL 1.830	SL LH 1.928
			II 1.744
M5	QW 1.657	QW 1.655	QW 1.640
			HH 1.770
	SL 1.765	SL 1.768	SL LH 1.795
			II 1.792
M6	QW 1.649	QW 1.655	QW 1.648
			HH 1.759
	SL 1.770	SL 1.756	SL LH 1.800
			II 1.817

with different thicknesses of the constituent layers from sample to sample. Our interest is twofold: On one hand, we wish to obtain more information on the superlattice band structure and on the GaAs/GaP band alignment from the transitions originating in the SL and in the QW, since both must be fitted with the same offset value. On the other hand, we wish to study the possibility of using the GaAs/GaP system for QW-based structures. The PL and PR spectra from these samples have behavior similar to that of samples M1, M2, and M3, but with the presence of a new transition originating in the QW. The superlattice in sample M4 has type-II behavior as described previously in samples M2 and M3. On the other hand, the superlattices in samples M5 and M6 have type-I behavior, analogous to sample M1.

In Table III the energies of the SL and QW observed in PL and PR spectra in these three samples are displayed.

In Fig. 5, we present a typical PL spectrum from sample M6 at 150 K. The peak labeled QW in the PL spectrum corresponds to the transition from the first confined QW state, and the peak labeled SL corresponds to the lowest su-

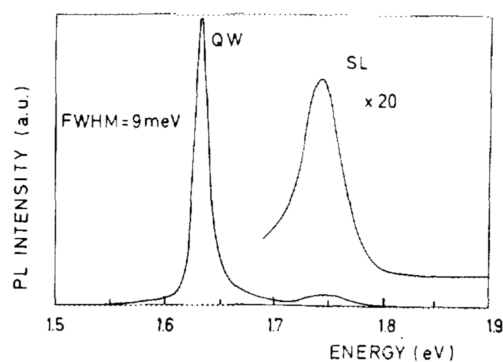

FIG. 5. PL spectrum from sample M6 (150 K). The quantum-well (QW) and superlattice (SL) transitions are clearly observed.

Downloaded 27 Jun 2012 to 161.111.180.103. Redistribution subject to AIP license or copyright; see http://jap.aip.org/about/rights_and_permissions

perlattice transition. It must be pointed out that, in spite of the broadness of the SL peak (the growth of GaAs/GaP by ALMBE is not yet optimized), the QW-related peak has a full width at half maximum (FWHM) of 9 meV, which implies that good-quality strained QW-based structures can be grown by ALMBE. Also, the PL intensity of the QW peak is comparable to that obtained in analogous structures where the two confining superlattices were short-period GaAs/AlAs.[12] This fact means that the charge transport to the QW, which takes place across the superlattice, has a high efficiency.

IV. THEORETICAL APPROACH

In this section we present the theoretical approach that has been used in the calculations. The goal is to obtain a good fit to all the type-I and type-II transitions observed in the different SL and QW whose parameters are given in Table I. The only adjustable parameter needed in the calculations is the band offset. This parameter has not been, as of yet, experimentally obtained and only some predictions have been made.[13,14]

GaAs/GaP being a strained-layer superlattice, a detailed consideration of the effects of strain on GaAs and GaP band structure is needed. In Fig. 6 a schematic description of the effects of the stress in the two constituent bulk materials is presented. In an unstrained zinc-blende-type material at the Γ point, the valence-band states are comprised of a fourfold $P_{3/2}$ multiplet ($J = 3/2$, $mj = \pm 3/2, \pm 1/2$) and a $P_{1/2}$ doublet ($J = 1/2$, $mj = \pm 1/2$). The application of a biaxial stress shifts $P_{3/2}$ and $P_{1/2}$ in energy with respect to the conduction band, splits the $P_{3/2}$ multiplet in two doublets ($J = 3/2, mj = \pm 3/2$ and $J = 3/2, mj = \pm 1/2$), and couples light-hole and split-off bands.[15]

Strain effects in the X states have to be taken into account for the type-II superlattices. Under a biaxial stress in the (001) plane the degeneracy of the three equivalent X minima in the [001], [010], and [100] directions is lifted, and the band is shifted as a whole[14] (see Fig. 6).

Deformation potentials have been taken for GaAs from Ref. 16 and for GaP from Ref. 17.

In order to describe the observed transitions we wanted a simple model that still accounted for the very strong valence-band mixing effects caused by stress.

Our starting point was the standard Kane model.[18] This model includes directly the coupling of the conduction band

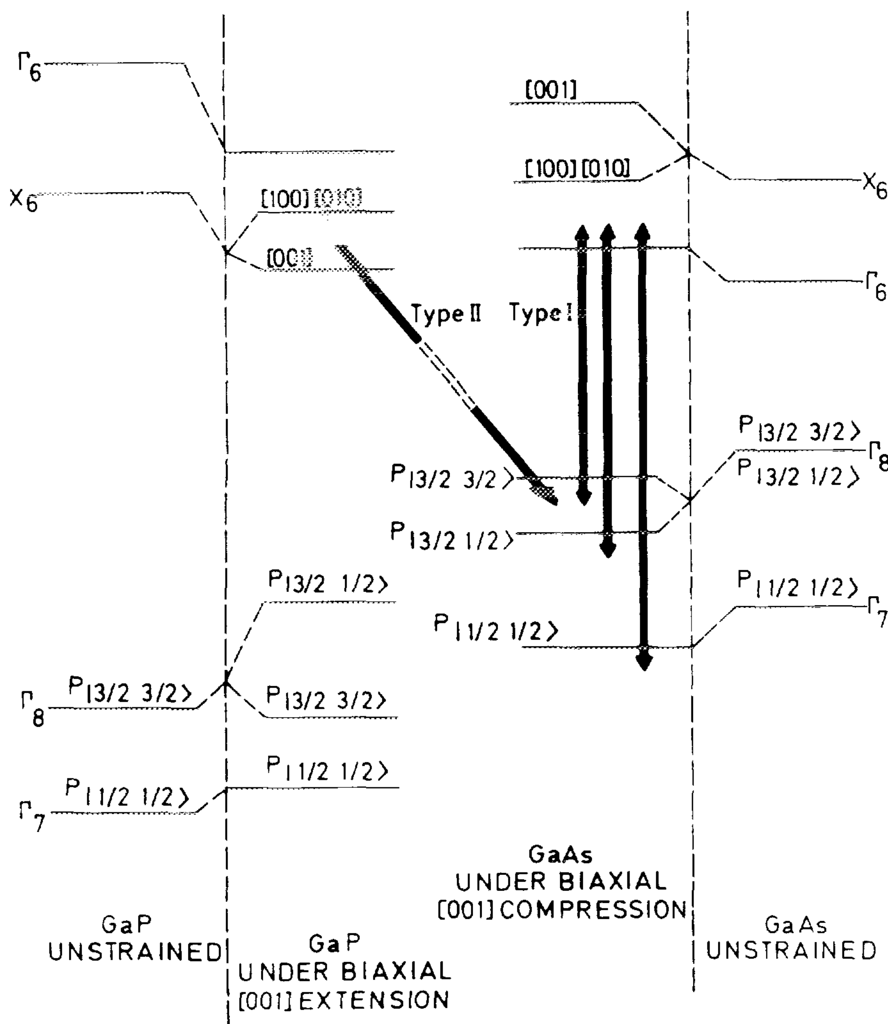

FIG. 6. Schematic band diagram of strained and unstrained GaAs and GaP. Arrows indicate the type-I and type-II transitions observable in the PR and PL spectra.

Downloaded 27 Jun 2012 to 161.111.180.103. Redistribution subject to AIP license or copyright; see http://jap.aip.org/about/rights_and_permissions

and heavy-hole, light-hole, and split-off bands, and perturbatively (via terms arising from Löwdin renormalization), the coupling of the remaining bands. A 4×4 matrix describes each bulk material in the $k_x = k_y = 0$ direction, in which the HH band is decoupled from the other bands.

The strain effects are incorporated by adding the stress-related matrix described in Ref. 15. The HH band is still decoupled and therefore can be treated separately, but the SO and LH bands are coupled by one Löwdin term and by a stress term. These terms could be neglected if they were much smaller than the spin-orbit splitting Δ. In the case of GaP, Δ is very small and thus the stress term must be retained in the model. Löwdin terms have been neglected in a model proposed by Marzin,[19] but we cannot do this in order to describe superlattice SO states without encountering singularities. However, a great simplification can still be achieved, following a treatment developed by Schuurmans and 't Hooft.[20] Both GaAs and GaP are large-band-gap materials, and the coupling of the CB with the LH or SO bands is much smaller than the coupling between the LH and SO bands, making a separate treatment of the CB possible.

Thus we end up with a Kronig–Penney type problem for the CB, with energy-dependent effective masses. Boundary conditions at the interfaces are the continuity of the CB-related envelope function and the continuity of its derivative divided by the corresponding effective mass. Separate Kronig–Penney calculations with analogous boundary conditions have been performed for superlattice states built with bulk X states, as has already been done for the AlAs/GaAs system.[21]

For the valence band, only Γ-related states are meaningful. The HH states are obtained in the same way as CB states but with constant effective masses, because they are decoupled from the other bands in z direction. The LH and SO bands are fully coupled, both in each material and by the boundary conditions, and thus our problem is not of Kronig–Penney type anymore. We obtain the SL states essentially as described in Ref. 20. Quantum-well states have been obtained in the same way as SL states.

In this calculation we do not take into account the nonlinear contribution to the deformation potential. A rough estimation can be done of the type-I transition dependence with those nonlinear strain terms. In particular, for sample M1 (with $\epsilon_{GaP} = 3.7\%$) the variation in the type-I transition energy induced by the nonlinearities is smaller than 5 meV.[22]

V. DISCUSSION

The transitions associated with the different peaks observed in the PL spectrum have been largely discussed in Sec. IV, identifying type-I and type-II transitions. In the PR spectra (samples M1, M2, and M3), as mentioned before, the peaks are too broad to resolve the conduction-band–light-hole transition from the conduction-band–heavy-hole transition. In the spectra in Fig. 4, peaks labeled SL correspond both to the light-hole and heavy-hole transitions. The spin-orbit transition is clearly observed in the three samples.

The only adjustable parameter in our calculations is the band offset. The comparison of experiments and theory is made for both type-I and type-II transitions. The sensitivity of the transition energy to the band-offset value is especially high for type-II transitions. A change in the offset has a small effect in both the confinement energy of the X-like conduction band and the lowest valence-band levels, because their effective masses are quite large (notice that, as shown in Tables II and III, the heavy-hole band is the lowest in our type-II superlattices). This implies that for a certain variation of the offset (see Fig. 6), the induced variation in type-II transitions has a magnitude analogous to the offset change. This is not the case of the type-I transitions where the variation in the transition energy induced by an offset modification is only due to the difference in confinement energies of electrons and holes. These arguments make the observation of type-II transition heterostructures a very accurate method for band-offset determination. This reasoning can be investigated by looking at the calculated type-I and type-II transitions for different offsets in Table II.

In comparing experimental and theoretical results, all the transitions must be properly fitted for a unique value of the band offset. In the calculations, the value of the conduction-band offset was varied in the range 0.1–1.1 eV. We have found the best fit to all the observed PL and PR transitions by using a conduction-band offset of 0.4 eV. This is to our knowledge the first direct determination of the band offset in the GaAs/GaP heterojunction, and the value obtained is close to the predictions of Refs. 13 and 14. In Table II, we present the energies of the transitions experimentally observed in samples M1, M2, and M3, together with the calculated ones, for three different conduction-band offsets around the final optimum choice of 0.4 eV. It must be emphasized how good the agreement between experiment and theory is, taking into account the simplicity of the theoretical model used.

The values of the heavy-hole and light-hole transition energies, as obtained in the calculation for an offset value of 0.4 eV, are marked in Fig. 4 by arrows for each superlattice. It must be noticed that the PR signal extends over the region in which both transitions are predicted theoretically in all three samples, which means that although not resolved experimentally, they contribute to the broad signal labeled SL in the spectra.

In Table III, all the superlattice and the QW-associated transition energies from samples M4, M5, and M6 are compared with the calculation using a conduction-band offset of 0.4 eV, and the agreement found confirms the choice made for the offset.

VI. CONCLUSION

We have studied the optical properties of a new mismatched system, the GaAs/GaP strained-layer superlattice, in which the lattice mismatch is 3.7%. By using an absorption-related technique (PR) and an emission-related technique (PL) we have been able to study, for the first time, type-I and type-II transitions in these strained superlattices, which show a behavior similar to that found for the lattice-matched GaAs/AlAs superlattices. The temperature and

Downloaded 27 Jun 2012 to 161.111.180.103. Redistribution subject to AIP license or copyright; see http://jap.aip.org/about/rights_and_permissions

excitation density dependence of the PL signal assured us of the assignment of the origin of the different peaks. Also, carrier transfer from the type-I to the type-II transition, assisted by a temperature increase, has been found for type-II superlattices. Calculations have been performed in order to fit all the transitions observed, with the only free parameter being the band offset. An optimum fit to all the observed transitions is found for a value of the conduction-band offset of 0.4 eV, which is the first estimation made from experimental measurements in this GaAs/GaP heterostructure.

ACKNOWLEDGMENTS

We would like to thank especially J. M. Rodriguez for PR measurements, A. Mazuelas for the x-ray information, and A. Ruiz for the growth of the samples. Also we thank C. Tejedor and G. Platero for interesting discussions on the theoretical aspects.

[1] J. Y. Marzin and J. M. Gerard, Superlattices Microstruct. 5, 51 (1989).
[2] P. L. Gourley, R. M. Biefeld, and P. B. Johnson, Appl. Phys. Lett. 51, 1310 (1987).
[3] N. El-Masry, J. C. L. Tarn, and T. P. Humphreys, Appl. Phys. Lett. 51, 20 (1987).
[4] E. Schirber, I. J. Fritz, and L. R. Dawson, Appl. Phys. Lett. 46, 187 (1985).
[5] P. L. Gourley and R. H. Biefeld, J. Vac. Sci. Technol. B 1, 383 (1983).
[6] M. Recio, J. L. Castaño, and F. Briones, Jpn. J. Appl. Phys. 27, 1204 (1988).
[7] G. Peter, E. O. Göbel, W. W. Rühle, J. Nagle, and K. Ploog, Superlattices Microstruct. 5, 197 (1989).
[8] G. Armelles, M. Recio, A. Ruiz, and F. Briones, Solid State Commun. 71, 431 (1989).
[9] A. Ruiz, L. González, and F. Briones, Appl. Phys. A (to be published).
[10] D. E. Aspnes and J. E. Rowe, Phys. Rev. Lett. 27, 188 (1971).
[11] K. Takahashi, T. Hayakawa, T. Suyama, M. Kondo, S. Yamamoto, and T. Hijikata, J. Appl. Phys. 63, 1729 (1988).
[12] F. Briones, L. González, M. Recio, and M. Vázquez, Jpn. J. Appl. Phys. 26, L1125 (1987).
[13] G. C. Osbourn, J. Appl. Phys. 53, 1587 (1982).
[14] C. Coluzza, F. Lama, A. Perfetti, C. Quaresima, and H. Capozi, J. Appl. Phys. 64, 3304 (1988).
[15] F. H. Pollak, Surf. Sci. 37, 863 (1973).
[16] M. Chandrasekhar and F. H. Pollak, Phys. Rev. B 15, 2127 (1977).
[17] H. Mathieu, P. Merle, E. L. Ameziane, B. Archilla, J. Camassel, and G. Poiblaud, Phys. Rev. B 19, 2204 (1979).
[18] E. O. Kane, in *Semiconductors and Semimetals*, edited by R. K. Willardson and A. C. Beer (Academic, New York, 1966), Vol. 1, pp. 75–100.
[19] J. Y. Marzin, in *Proceedings of the Winter School on Heterojunctions and Semiconductor Superlattices*, edited by G. Allan, G. Bastard, N. Boccara, N. Lannoo, and M. Voos (Springer, Berlin, 1986), pp. 161–176.
[20] M. F. H. Schuurmans and G. W. 't Hooft, Phys. Rev. B 31, 8041 (1985).
[21] E. Finkman, M. D. Sturge, M.-H. Meynadier, R. E. Nahory, M. C. Tamargo, D. M. Hwang, and C. C. Chang, J. Lumin. 39, 57 (1987).
[22] G. Armelles and M. Recio (unpublished).

Downloaded 27 Jun 2012 to 161.111.180.103. Redistribution subject to AIP license or copyright; see http://jap.aip.org/about/rights_and_permissions